Assessing the Effects of LSS Choice on Simulated Geopotential Heights over China: A Case Study Using WRF

Xin-Min Zeng*, B. Wang, Y. Zhang, and N. Wang

College of Hydrology and Water Resources, Hohai University, Nanjing 210098, China

Contact: xinmin.zeng@hhu.edu.cn

The 98th AMS annual Meeting, Austin, TX, January 7-11, 2018

Abstract

To quantify and explain effects of different land surface schemes (LSSs) on simulated geopotential height (GPH) fields, we performed simulations over China for the summer of 2003 using 12-member ensembles with the Weather Research and Forecasting Model (WRF), Version 3. The results show that while the model can generally simulate the seasonal and monthly mean GPH patterns, the effects of the LSS choice on simulated GPH fields are substantial, with the LSS-induced differences exceeding 10 gpm over a large area (especially the Northwest) of China, which is very large compared with climate anomalies and forecast errors. In terms of the assessment measures for the four LSS ensembles (namely, SLAB, NOAH, RUC, and PLEX) in the WRF, the PLEX ensemble is the best, followed by the NOAH, RUC, and SLAB ensembles. The sensitivity of the simulated 850-hPa GPH is more significant than that of the 500-hPa GPH, with the 500-hPa GPH difference fields generally characterized by two large areas with opposite signs due to the smoothly varying nature of GPHs. LSS-induced GPH sensitivity is found to be higher than the GPH sensitivity induced by atmospheric boundary layer schemes. Moreover, theoretical analyses show that the LSS-induced GPH sensitivity is mainly caused by changes in surface fluxes (in particular, sensible heat flux), which further modify atmospheric temperature and pressure fields. The temperature and pressure fields generally have opposite contributions to changes in the GPH. This study emphasizes the importance of choosing/improving LSSs for simulating/forecasting seasonal and monthly GPHs (therefore precipitation) using regional climate models.

Methodology

Model and experimental design

- The Advanced Research WRF (ARWv3) model (Skamarock et al. 2008)
- Four LSSs (12-member ensemble simulations): (1) the five-layer thermal diffusion scheme (SLAB; Dudhia 1996); (2) the Noah LSS (NOAH; Chen and Dudhia 2001; Ek et al. 2003); (3) the Rapid Update Cycle LSS (RUC; Smirnova et al. 1997, 2000); and (4) the Pleim-Xiu LSS (PLEX; Xiu and Pleim 2001)
- Additionally, four PBLSs (12-member ensemble simulations): (1) the Yonsei University scheme (YSUbl; Hong et al. 2006), (2) the modified Mellor-Yamada scheme (MYJbl; Mellor and Yamada 1982; Janjic, 2001), (3) the Quasi-Normal Scale Elimination model (QNSEbl; Sukoriansky et al. 2006), and (4) the PBLS of the asymmetric convective model, version 2 (ACM2bl; Pleim 2007)
- All of these simulations were carried out for the approximate period of May 1 through September 1, 2003, and each simulation is a slightly perturbed, 12-member ensemble with initial conditions chosen at 0000, 0600, 1200 and 1800 UTC 1-3 May 2003, to make the simulation results more robust. The four-month (MJJA) integrations were performed using the first month integration taken as a model spin-up, and we used the JJA results for analysis.

Data

- For the initial and boundary conditions of the simulations, the NCEP 1°×1° Final (FNL) Analysis data are used. Because the horizontal resolution of 30 km in this study is much higher, also employed are the 38-km NCEP Climate Forecast System Reanalysis (CFSR) data (http://cfs.ncep.noaa.gov/cfsr/) for the comparison
- Conventional radiosonde GPH data (available at 00 and 12 UTC each day during the summer of 2003) are used for validation

Atmospheric equation for GPH change

Contributions to the GPH changes from the changes in air temperature and surface pressure can be derived for various levels (e.g., 850 and 500 hPa):

For 850 hPa:

$$\int_{p_s}^{p_{850}} \frac{dp}{p} = -\int_{H_s}^{H_{850}} \frac{g^*}{RT} dH, \qquad \delta H_{850} \approx H_{850}\frac{\delta \overline{T}}{\overline{T}} + 6.15 H_{850}\frac{\delta p_s}{p_s}$$

For 500 hPa:

$$\delta H_{500} \approx H_{500}\frac{\delta \overline{T}}{\overline{T}} + 1.44 H_{500}\frac{\delta p_s}{p_s}$$

The finite differential values in the equations can be regarded as the perturbations induced by the LSSs, and the contributions to the GPH changes from the changes in air temperature and surface pressure can be obtained.

Results

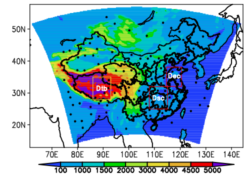

FIG. 1. Topographic elevations (unit: m) and spatial distribution of selected observational stations within the model domain. The sub-areas denoted as "D_{tb}" (86°-93°E; 28°-35°N), "D_{sc}" (108°-115°E, 25°-32°N), and "D_{ec}" (115°E-120°E, 32°N-38°N) are used in section 4.d.

TABLE 1. Ensemble mean seasonal CORR, BIAS, RMSE, STD_m, and STD_m-STD_o for the LSS-simulated evapotranspiration over land, where observations are from Miralles et al. (2013), and STD_o =0.87 mm d^{-1}.

	CORR	BIAS	RMSE	STD_m	STD_m-STD_o
	(---)	(mm d^{-1})	(mm d^{-1})	(mm d^{-1})	(mm d^{-1})
SLAB	0.51	0.17	1.19	1.35	0.48
NOAH	0.73	-0.03	0.85	1.24	0.37
RUC	0.55	-0.43	0.97	0.94	0.07
PLEX	0.70	0.68	1.24	1.45	0.58

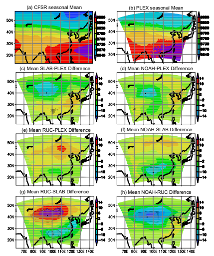

FIG. 2. Ensemble and seasonal mean GPH distributions at 500 hPa for 00 UTC (unit: gpm), where regions with significant LSS-induced differences are marked with grey and black dots, and grey (black) dots indicate the ensemble-mean GPH differences that are significant at the 5% (10%) level, according to the t test for the time series of daily GPH values of the study period.

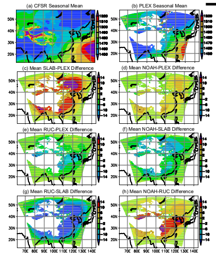

FIG. 3. Same as Fig. 2 but for 850 hPa..

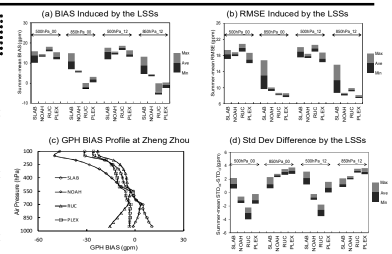

FIG. 3. Ensemble results of (a) BIAS, (b) RMSE, (c) GPH BIAS profiles at Zheng Zhou station (113.65ºE, 34.72ºN), and (d) the difference of the standard deviation of the summer mean GPHs over China at 500 and 850 hPa for 00 and 12 UTC, where the "Ave", "Max", and "Min" levels in the shaded bars denote the 12-member ensemble mean, maximum, and minimum, respectively..

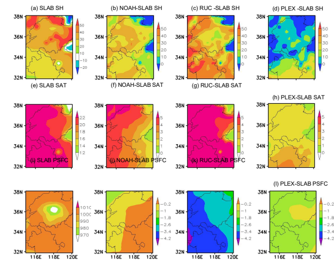

FIG. 4. Ensemble-mean seasonal SLAB means and differences between SLAB and the other LSSs. (a) SLAB sensible heat flux (units: W m^{-2}). (b) Difference in sensible heat flux between NOAH and SLAB (NOAH minus SLAB). (c) As shown in (b) but for RUC minus SLAB. (d) As shown in (b) but for PLEX minus SLAB. (e) As shown in (a) but for SLAB surface air temperature (units: ˚C). (f) As shown in (e) but for NOAH minus SLAB. (g) As shown in (e) but for RUC minus SLAB. (h) As shown in (e) but for PLEX minus SLAB. (i) As shown in (a) but for SLAB surface pressure (units: hPa). (j) As shown in (i) but for NOAH minus SLAB. (k) As shown in (i) but for RUC minus SLAB. (l) As shown in (i) but for PLEX minus SLAB.

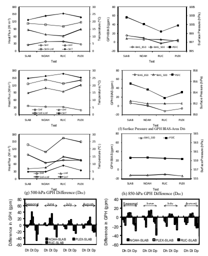

FIG. 5. Ensemble LSS-induced means for the three subareas (Fig. 1): (a) sensible heat flux (SHF), land heat flux (LHF), the sum of SHF and LHF, and SAT for the Dec subarea; (b) 850- and 500-hPa GPH BIASs and surface air pressure for Dec; (c) same as (a) for Dsc; (d) same as (b) for Dsc; (e) same as (a) for Dtb; (f) same as (b) for Dtb; (g) 500-hPa GPH differences, where $D_h = \delta H_{500}$, $D_t = H_{500}$, and D_p =1.44 H_{500} ; and (h) 850-hPa GPH differences, where $D_h = \delta H_{850}$, $D_t = H_{850}$, and D_p =6.15 H_{850} (unit: gpm).

Summary

- Different LSSs produce geopotential height fields that could be systematically, and statistically and significantly different.
- The LSS-induced GPH sensitivity is mainly caused by changes in surface fluxes (in particular, sensible heat flux), which further leads to opposite contributions of modified atmospheric temperature and pressure fields.
- Choosing/improving LSSs for simulating seasonal and monthly GPHs (or atmospheric circulation) using regional climate models is of importance.

Acknowledgement: This research was funded by the National Natural Science Foundation of China (Grant Nos. 41675007 and 41475063) and the Fundamental Research Funds for the Central Universities (Grant No. 2017B06214). This is also a contribution to JHM, and we thank those who provided helpful comments and suggestions.